Performance comparison of 40 Gb/s ULH transmissions using CSRZ-ASK or CSRZ-DPSK modulation formats on UltraWave™ fiber

E. Pincemin,[1*] A. Tan,[1] A. Tonello,[2,6] S. Wabnitz,[2] J.D. Ania-Castañón,[3] V. Mezentsev,[3] S. Turitsyn,[3] Y. Jaouën,[4] L. Grüner-Nielsen[5]

[1]*France Telecom, Research & Development Division, Technopôle Anticipa, 2 Avenue Pierre Marzin, 22307 Lannion Cedex, France*

[2]*Institut Carnot de Bourgogne, UMR CNRS 5209, 9 Avenue Alain Savary 21078 Dijon, France*

[3]*Photonics Research Group, School of Engineering and Applied Science, Aston University Birmingham B4 7ET, UK*

[4]*GET / Telecom Paris, CNRS UMR 5141, 46 rue Barrault, 75634 Paris Cedex, France*

[5]*OFS Fitel Denmark, Priorparken 680, DK-2605 Brondby, Denmark*

[6]*Current address : XLIM, Département Photonique, UMR CNRS 6172, 123 Avenue Albert Thomas, 87060 Limoges, France*

[*]*Corresponding author: erwan.pincemin@orange-ftgroup.com*

Abstract: In this work we present extensive comparisons between numerical modelling and experimental measurements of the transmission performance of either *CSRZ-ASK* or *CSRZ-DPSK* modulation formats for 40-Gb/s *WDM ULH* systems on UltraWave™ fiber spans with all-Raman amplification. We numerically optimised the amplification and the signal format parameters for both *CSRZ-DPSK* and *CSRZ-ASK* formats. Numerical and experimental results show that, in a properly optimized transmission link, the *DPSK* format permits to double the transmission distance (for a given *BER* level) with respect to the *ASK* format, while keeping a substantial *OSNR* margin (on *ASK* modulation) after the propagation in the fiber line. Our comparison between numerical and experimental results permits to identify what is the most suitable *BER* estimator in assessing the transmission performance when using the *DPSK* format.

OCIS codes: (060.4080) Modulation; (060.4510) Optical communications; (190.4370) Nonlinear optics, fibers.

References and links

1. "Mintera achieves record ultra long haul transmission distance at 40 Gb/s", March 2002; "Migrating to 40-Gbit/sec DWDM networks," FibreSystems Europe, September 2002, www.mintera.com.
2. "Lucent Technologies ships its new, industry-leading optical system - LambdaXtreme™ transport - to Deutsche Telekom," Lucent press release, March 2002, www.lucent.com
3. "Lambdaxtreme™ Transport successfully completes field trial in Deutsche Telekom network," Lucent press release, July 2002, www.lucent.com.
4. "CoreStream Agility Optical Transport system data sheet," January 2007, www.ciena.com.
5. "Alcatel 1626 Light Manager data sheet," January 2007, www.alcatel-lucent.com.
6. "MCI, Xtera, Mintera, and Juniper Networks Show High-Bandwidth Optical Technology Capable of Reaching Farther Distances over Existing Fiber Networks," FibreSystems Europe, December 2005, www.mintera.com.
7. "40G moves back onto the agenda," FibreSystems Europe, May 2004, www.strataligtht.com.
8. B. Zhu, L. E. Nelson, L. Leng, M. O. Pedersen, D. W. Peckham, and S. L. Stulz, "Transmission of 1.6 Tb/s (40 x 42.7 Gb/s) Over Transoceanic Distance with Terrestrial 100-km Amplifier Spans," in *Optical Fiber Communication Conference*, Technical Digest (Optical Society of America, 2003), paper FN2. http://www.opticsinfobase.org/abstract.cfm?URI=OFC-2003-FN2.

#82382 - $15.00 USD Received 24 Apr 2007; revised 4 Jul 2007; accepted 15 Jul 2007; published 21 Aug 2007

9. B. Zhu, L. Nelson, L. Leng, S. Stulz, S. Knudsen, D. Peckham, " 1.6 Tb/s (40 x 42.7 Gb/s) transmission over 2400 km of fibre with 100-km dispersion-managed spans," Electron. Lett. **38**, 647-648 (2002).
10. C. Rasmussen, T. Fjelde, J. Bennike, F. Liu, S. Dey, B. Mikkelsen, P. Mamyshev, P. Serbe, P. Van Der Wagt, Y. Akasaka, D. Harris, D. Gapontsev, V. Ivshin, P. Reeves-Hall, "DWDM 40 Gb/s Transmission over Transpacific distance (10000 km) using CSRZ-DPSK, enhanced FEC, and All-Raman amplified 100-km Ultrawave fiber spans," J. Lightwave Technol. **10**, 281-293 (2004).
11. B. Zhu, L. E. Nelson, S. Stulz, A. H. Gnauck, C. Doerr, J. Leuthold, L. Gruner-Nielsen, M. O. Pedersen, J. Kim, R. Lingle, Y. Emori, Y. Ohki, N. Tsukiji, A. Oguri, and S. Namiki, "6.4-Tb/s (160 x 42.7 Gb/s) transmission with 0.8 bit/s/Hz spectral efficiency over 32 x 100 km of fiber using CSRZ-DPSK format," in *Optical Fiber Communication Conference*, Technical Digest (Optical Society of America, 2003), paper PD19.
http://www.opticsinfobase.org/abstract.cfm?URI=OFC-2003-PD19.
12. T. Tsuritani, K. Ishida, A. Agata, K. Shimomura, I. Morita, T. Tokura, H. Taga, T. Mizuochi, and N. Edagawa, "70GHz-spaced 40 x 42.7Gbit/s transmission over 8700km using CS-RZ DPSK signal, all-Raman repeaters and symmetrically dispersion-managed fiber span," in *Optical Fiber Communication Conference*, Technical Digest (Optical Society of America, 2003), paper PD23.
http://www.opticsinfobase.org/abstract.cfm?URI=OFC-2003-PD23.
13. B. Zhu, L. Leng, A. H. Gnauck, M. O. Pedersen, D. Peckham, L. E. Nelson, S. Stulz, S. Kado, L. Grüner-Nielsen, R. L. Lingle, S. Knudsen, J. Leuthold, C. Doerr, S. Chandrasekhar, G. Baynham, P. Gaarde, Y. Emori, and S. Namiki, "Transmission of 3.2 Tb/s (80 x 42.7 Gb/s) over 5200 km of UltraWave fiber with 100-km dispersion managed spans using RZ-DPSK format," in *proceedings ECOC'2002*, DK, Copenhaguen, paper PD4.2.
14. C. Rasmussen, S. Dey, F. Liu, J. Bennike, B. Mikkelsen, P. Mamyshev, M. Kimmitt, K. Springer, D. Gapontsev, and V. Ivshin, "Transmission of 40x42.7 Gb/s over 5200 km ultraWave fiber with terrestrial 100 km spans using turn-key ETDM transmitter and receiver," in *proceedings ECOC'2002*, DK, Copenhaguen, paper PD4.4.
15. C. J. Rasmussen, T. Fjelde, J. Bennike, F. Liu, S. Dey, B. Mikkelsen, P. Mamyshev, P. Serbe, P. van der Wagt, Y. Akasaka, D. Harris, D. Gapontsev, V. Ivshin, and P. Reeves-Hall, "DWDM 40G transmission over trans-Pacific distance (10,000km) using CSRZ-DPSK, enhanced FEC and all-Raman amplified 100km UltraWave™ fiber spans," in *Optical Fiber Communication Conference*, Technical Digest (Optical Society of America, 2003), paper PD18.
http://www.opticsinfobase.org/abstract.cfm?URI=OFC-2003-PD18.
16. T. Hoshida, O. Vassilieva, K. Yamada, S. Choudhary, R. Pecqueur, H. Kuwahara, "Optimal 40 Gb/s modulation formats for spectrally efficient long-haul DWDM systems," J. Lightwave Technol. **20**, 1989-1996 (2002).
17. A. H. Gnauck, G. Raybon, S. Chandrasekhar, J. Leuthold, C. Doerr, L. Stulz, A. Agarwal, S. Banerjee, D. Grosz, S. Hunsche, A. Kung, A. Marhelyuk, D. Maywar, M. Movassaghi, X. Liu, C. Xu, X. Wei, and D. M. Gill, "2.5 Tb/s (64x42.7 Gb/s) transmission over 40x100 km NZDSF using RZ-DPSK format and all-Raman-amplified spans," in *Optical Fiber Communications Conference*, A. Sawchuk, ed., Vol. 70 of OSA Trends in Optics and Photonics (Optical Society of America, 2002), paper FC2.
18. J.D. Ania-Castañón, I.O. Nasieva, N. Kurukitkoson, S.K. Turitsyn, C. Borsier, E. Pincemin, "Nonlinearity management in fiber transmission systems with hybrid amplification," Opt. Commun. **233,** 353 (2004).
19. A. Judy, "Dispersion Managed Spans in Terrestrial Routes: Technical Advantages and Practical Considerations," in *Optical Fiber Communication Conference*, Technical Digest (Optical Society of America, 2003), paper TuS1.
http://www.opticsinfobase.org/abstract.cfm?URI=OFC-2003-TuS1
20. C. Xu, X. Liu, X. Wei, "DPSK for high spectral efficiency optical transmissions," J. Selected Topics Quantum Electron. **10**, 281-293 (2004).
21. X. Wei, X. Liu, "Analysis of intrachannel four-wave mixing in differential phase-shift keying transmission with large dispersion," Opt. Lett. **28**, 2300-2302 (2003).
22. R. I. Killey, H. J. Thiele, V. Mikhailov, and P. Bayvel, "Reduction of intrachannel nonlinear distortion in 40-Gb/s-based WDM transmission over standard fiber," IEEE Photon. Technol. Lett. **12**, 1624–1626 (2000).
23. E. Pincemin, D. Grot, C. Borsier, J.D. Ania-Castañòn, S.K. Turitsyn, "Impact of the fiber type and dispersion management on the performance of an NRZ 16x40 Gb/s DWDM transmission system," IEEE Photon. Technol. Lett. **16**, 2362–2364 (2004).
24. J. P. Gordon and L. F. Mollenauer, "Phase noise in photonics communications systems using linear amplifier," Opt. Lett. **15**, 1351–1355 (1990).
25. D. Marcuse, "Derivation of analytical expressions for the bit-error probability in lightwave systems with optical amplifiers," J. Lightwave Technol. **8**, 1816-1823 (1990).
26. P. A. Humblet and M. Azizoglu, "On the bit error rate of lightwave systems with optical amplifiers," J. Lightwave Technol. **9**, 1576–1582 (1991).
27. A. Richter, I. Koltchanov, K. Kuzmin, E. Myslivets, and R. Freund, " Issues on Bit-Error Rate Estimation for Fiber-Optic Communication Systems," in *Optical Fiber Communication Conference and Exposition and The National Fiber Optic Engineers Conference*, Technical Digest (CD) (Optical Society of America,

#82382 - $15.00 USD Received 24 Apr 2007; revised 4 Jul 2007; accepted 15 Jul 2007; published 21 Aug 2007

2005), paper NTuH3.
http://www.opticsinfobase.org/abstract.cfm?URI=NFOEC-2005-NTuH3
28. M.K. Liu, A.C. Vrahas, M.J.B. Moretti, "Saddle point bit error rate computations for optical communication systems incorporating equalizers," IEEE Trans. Commun. **43**, 989-1000 (1995).
29. "CHROMOS11 optical network chromatic dispersion and PMD test set data sheet," September 2005, www.pefiberoptics.com.

1. Introduction

In spite of their availability since a few years as commercial products, 40 Gb/s optical transmission systems have not yet been extensively deployed in the field by carriers [1-3]. The main reason for this delay was the competition from ultra long-haul (*ULH*) 10 Gb/s *WDM* transmission systems, whose mature technology enabled maximum transmission distances well beyond 2000 km, without electronic regeneration [4-5]. At present however there is a renewed interest in the deployment of 40 Gb/s transport solutions, thanks to transponder technology advances and the associated cost reductions. As a consequence, it is expected that upgrading *ULH* transmission systems to a 40 Gb/s per channel granularity will enable further cost savings [6-7]. A crucial issue for carriers intending to deploy 40 Gbit/s systems is to be able to perform a critical evaluation of the performances of *ULH* 40 Gb/s WDM transmission systems when introducing innovative fiber bases (such as the UltraWave^{TM} fiber), which have been specially designed for enabling 40 Gb/s transmissions on more than 2000 km [8-15], when used in combination with advanced modulation formats [8-17, 20-22].

In this work we present, we believe for the first time, a detailed numerical and experimental inter-comparison of ULH 40 Gbit/s WDM system performance, using either the *CSRZ-ASK* or the *CSRZ-DPSK* modulation format [8-17, 20-22] over exactly the same link configuration of UltraWave^{TM} fiber spans [8-15]. In other words, in order to ensure a fair comparison of the system performance when using the two different modulation formats, we kept unchanged throughout the experiments both the fiber base (and the dispersion map), as well as the amplifier configuration. Moreover, we guided our experiments by means of extensive numerical simulations, in order to point out the contribution of the major sources of transmission penalty, and to determine the optimal signal and link configuration. For the *DPSK* format, we compared the experimental bit-error-rate (*BER*) with the predictions of different Q-factor estimators (such as the amplitude Q-factor [25-26], the differential-phase Q-factor [20], as well as the semi-stochastic *BER* estimation using moment generating functions and the saddle point approximation [27-28]). In this way, we could determine which *BER* estimator is best suited to predict the experimentally observed *BER*, as well as the optimal system configuration. Transmission losses were compensated by bi-directional all-Raman distributed amplification: the corresponding optimal amplifier configuration (i.e., the ratio between forward and backward Raman gain) was determined by means of the nonlinearity management approach [18]. On the other hand, for each modulation format we independently optimized the span input power per channel, as well as the pre- and the post-compensation: as we shall see, the numerical and experimental optimization results are in good agreement.

2. Experimental set-up

Our experimental set-up is shown in Fig. 1. The transmitter involved sixteen *DFB* laser sources, ranging from 1544.53 nm to 1556.56 nm on a 100-GHz *ITU*-grid. Odd and even channels were separately multiplexed, independently modulated, combined and co-polarized through a polarization maintaining 3-dB coupler. Each transmitter was composed of two cascaded external $LiNbO_3$ Mach-Zehnder modulators.

The first modulator was used for either amplitude or phase modulation, when biased at the transmission mid or null-point, respectively. This modulator was driven by a 40-Gb/s pseudo-random bit sequence (*PRBS*) of 2^{31}-1 bit length. The second modulator was biased at the

#82382 - $15.00 USD Received 24 Apr 2007; revised 4 Jul 2007; accepted 15 Jul 2007; published 21 Aug 2007

transmission null-point, and it was driven by a 20 GHz clock for generating the 40-GHz *RZ* train with a 66% duty cycle. The different *WDM* channels were transmitted through a pre-compensation fiber, amplified by an Erbium-doped fiber amplifier (*EDFA*), and injected into the loop.

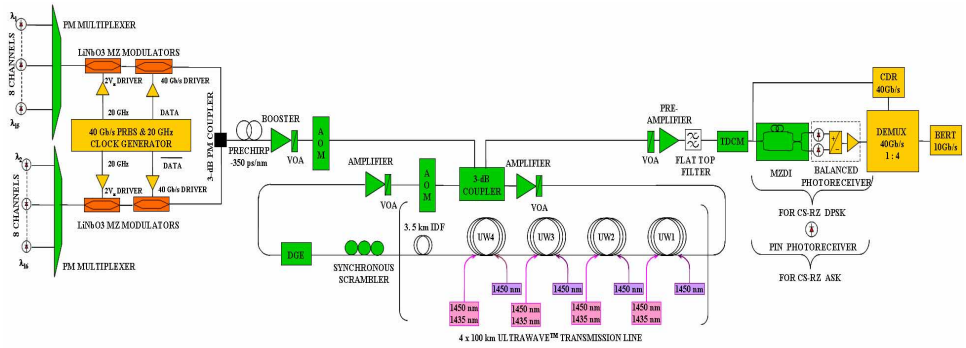

Fig 1. Schematic of the experimental set-up.

In Fig. 2 we illustrate the temporal and spectral properties of our transmitter for each of the two modulation formats under test. In the left column of Fig. 2 we show the eye diagrams as measured by means of an oscilloscope equipped with a 65 GHz optical sampling module and a high-precision time base. In the right column of Fig. 2 we show the signal optical spectra from an optical spectrum analyser with 10 pm resolution bandwidth. The small residual carrier in the CSRZ-ASK spectrum of Fig. 2 is due to the imperfect modulator response.

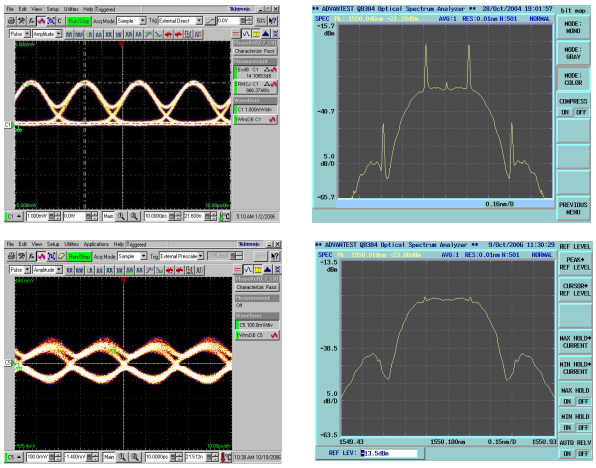

Fig 2. Temporal and spectral characterization of our transmitters: *CSRZ-ASK* (top), *CSRZ-DPSK* (bottom).

As shown in Fig.1, the re-circulating loop contained four 100-km dispersion-managed fiber (*DMF*) spans of *SLA-IDF-SLA* UltraWave™ fiber [8-15]. The *SLA* and *IDF* fibers at 1550 nm had a loss of 0.18 and 0.235 dB/km, a chromatic dispersion of 20 and -40 ps/nm/km, and an effective area of 107 and 31 μm², respectively [19]. Each span involved a symmetrical fiber arrangement, namely: 34 km of *SLA*, 32 km of *IDF*, and 34 km of *SLA*. Figure 3

#82382 - $15.00 USD Received 24 Apr 2007; revised 4 Jul 2007; accepted 15 Jul 2007; published 21 Aug 2007

illustrates the details of the dispersion map over the two first circulations in the loop. The residual span cumulated dispersion was of about 40 ps/nm at 1550 nm. Therefore we inserted after the four transmission spans an additional 3.5 km of *IDF*, in order to bring back the loop cumulated dispersion to ~0 ps/nm. Note that the experimental loop cumulated dispersion was affected by contributions from the different devices. Therefore it was necessary to accurately measure the residual loop cumulated dispersion by means of a custom designed set-up [29], yielding the value of 40 ps/nm. The dispersion measurement set-up implemented the differential phase shift method, where a monochromatic tuneable light source is used as transmitter. The same measurement set-up (using this time the fixed analyser method) also permitted us to determine the net polarization mode dispersion (*PMD*) (or average differential group delay (DGD)) in the loop. We obtained a loop *PMD* value close to 1 ps, whereas the nominal span *PMD* was equal to 0.04 ps/km$^{1/2}$. In order to minimize the loop-induced polarization effects, we used a polarisation scrambler, which was synchronously modulated with the loop circulation period. The cumulated loss of each fiber span of 22.5 dB (including splices, pump-signal *WDM* multiplexers and connectors) was fully compensated by means of bi-directional distributed Raman amplification.

As discussed in more details in the next section, the numerical optimization of the all-Raman amplification scheme [16] in the UltraWave^{TM} spans suggested the forward and backward Raman gain values of 4.5 and 18 dB, respectively. Such gains were obtained by means of a forward pump at 1455 nm, and a backward pump at 1435 and 1455 nm, respectively. In addition, a dynamic gain equalizer (*DGE*) was used in order to achieve loop gain equalization, and to suppress amplified spontaneous emission noise outside the signal band. We further inserted in the loop two additional *EDFA*s. The first *EDFA* permitted us to adjust the input power level into the first span (and subsequent ones). Whereas the second *EDFA* was used in order to compensate for the losses of the *IDF*, of the various other devices in the loop, such as *DGE*, the loop acousto-optic switch, the 3-dB loop coupler and the polarization scrambler.

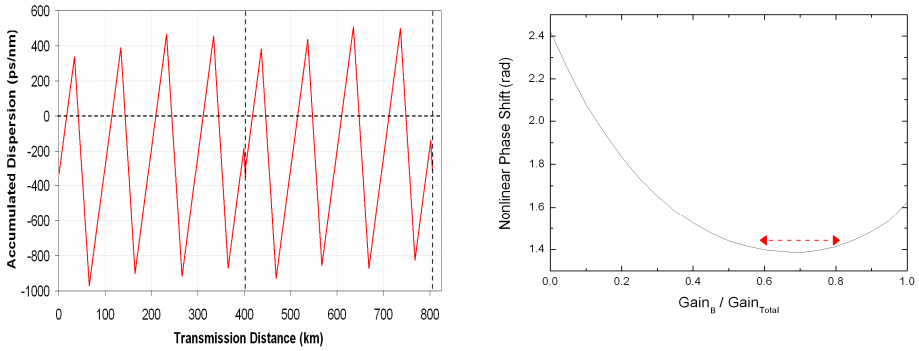

Fig 3. Left: Dispersion map on the first two loop round-trips for the channel at 1550 nm. Right: Theoretical nonlinear phase shift versus the ratio of backward to total Raman gain.

After a pre-determined number of circulations, the channel under measurement was selected by means of a square flat-top optical filter with the 20-dB bandwidth of 0.7 nm. The optimization of the filter bandwidth was performed in back-to-back configuration, and led to the same results for both the *CSRZ-ASK* and the *CSRZ-DPSK* modulation formats. The value of post-compensation was also optimized by means of a tuneable dispersion compensation module (*TDCM*) for each configuration under test [19]. Finally, the *CSRZ-ASK* signal was detected by a PIN photodiode and fed into a 40-Gb/s 1:4 electrical time division de-multiplexer (*ETDM*). For the *DPSK* format, before detection, the optical signal was

#82382 - $15.00 USD Received 24 Apr 2007; revised 4 Jul 2007; accepted 15 Jul 2007; published 21 Aug 2007

demodulated by a Mach-Zehnder 1-bit delayed fiber interferometer (*MZDI*). A balanced PIN photodiode circuit acted as the *DPSK* detector. After the *ETDM*, the average *BER* of the four 10-Gb/s tributaries was determined. Indeed, due to the loop operation, the *BER* was randomly measured on each of the four 10 Gb/s tributaries, for every signal burst that was sent to the *BER* tester.

3. Simulation results

In this section we describe an extensive set of numerical simulations, carried out with the purpose of supporting the experiments with design guidelines for the many independent link and signal parameters. Indeed, a careful optimization and fine tuning are required for both the Raman amplifier, as well as for the dispersion map configuration and the input signal power level. First of all, we identified the most appropriate ratio of forward to backward Raman gains. To this end, we applied a previously described general Raman amplifier optimization procedure, which is based on the mean-field approximation and the Raman power evolution equations [18]. In this way, we could predict that the nonlinear transmission impairments can be minimized (for any desired level of the output optical signal-to-noise ratio) whenever the Raman pumping is such that the backward pump provides between 60% and 80% of the total Raman gain (see Fig. 3, right hand side). We could confirm this prediction by means of full (that is, without the mean-field approximation) numerical simulations involving the transmission of a comb of modulated *WDM* channels. More precisely, modulated signal transmission simulations show that the best system performance is obtained whenever 80% of the total gain is provided by the backward pump, and the remaining 20% by the forward pump. As a result, in our experiments we retained the 20% forward-80% backward pump ratio for both the *CSRZ-ASK* and the *CSRZ-DPSK* formats.

We performed a numerical optimisation of the dispersion map and of the input signal power level per channel. For each of the two modulation formats under study, we evaluated the dependence of Personick's *Q* factor, evaluated at a balanced receiver (for the central channel in a comb of 5 *WDM* channels with 100 GHz spacing), as a function of both the signal pre-compensation (or prechirp) and the net residual loop dispersion (as discussed in section 2). Figure 4 shows the various levels of constant output *Q* factor versus both pre and residual dispersion. The right plot in Fig. 4 was obtained after transmission through a 4000 km UltraWave^{TM} fiber link with the *CSRZ-DPSK* format: as it can be seen, for residual loop dispersions higher than 20 ps/nm the pre-compensation should be reduced below -200 ps/nm. In particular, for the experimentally measured residual dispersion of 40 ps/nm (see section 2), Fig. 4 (right) predicts that the optimal pre-compensation should be equal to about -300 ps/nm. This value is very close to the actual optimal pre-compensation as it was determined in the experiments. The plots of Fig. 4 show that, with either *ASK* or *DPSK* modulation formats, pre-compensation should be a negative, linearly decreasing function of residual loop dispersion. Note that, although we used a nearly symmetrical dispersion map, the knowledge of the effective net residual dispersion per loop is a key element for determining the optimal pre-compensation value.

Next, Fig. 5 shows the dependence of the output *Q* factor (as in Fig. 4, the *Q* factor is evaluated for the central channel when propagating a comb of 5 *WDM* channels with 100 GHz spacing) as a function of pre-compensation and input channel power in the UltraWave^{TM} fiber spans. In the simulations of Fig. 5, we fixed the value of the residual loop dispersion to 40 ps/nm, which again corresponds to the measured value in our experimental setup. The white dots in the plots of Fig. 5 indicate the experimental optimal working points. Figure 5 shows that, for both the *ASK* and the *DPSK* modulation formats, the simulations predict optimal pre-compensation and channel input powers which turn out to be in good quantitative agreement with the corresponding experimental optimal values. In the simulations leading to Fig. 4 and 5, the optimization of the dispersion map and of the *CSRZ-DPSK* signal power was based on the evaluation of Personick's signal quality *Q* factor as it is measured by a balanced

#82382 - $15.00 USD Received 24 Apr 2007; revised 4 Jul 2007; accepted 15 Jul 2007; published 21 Aug 2007

detector. On the other hand, the experimental optimization of the *CSRZ-DPSK* transmissions was carried out by minimizing the bit-error-rate (*BER*) at the balanced receiver. As it is well known, with the *DPSK* format the simple relationship $BER = (1/2)\, Erfc\left[Q/\sqrt{2} \right]$ does not hold between the value of *Q* and the corresponding *BER* [27].

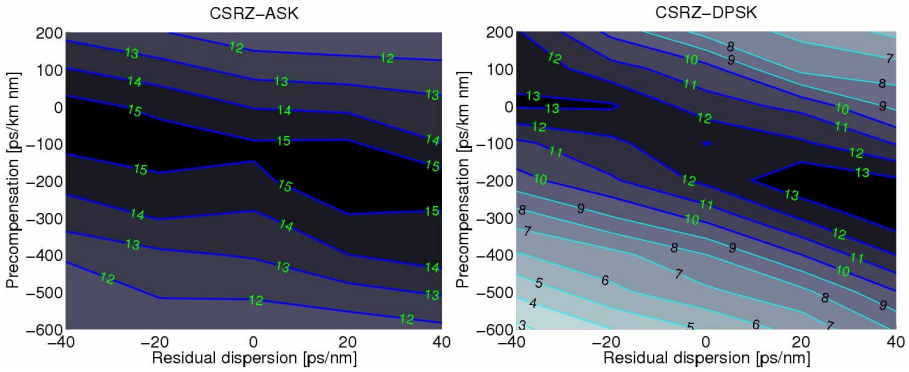

Fig 4. Left: numerical estimation of the output *Q* factor [dB] as a function of the pre-compensation and of the residual loop dispersion for a transmission over 2000 km using the *CSRZ-ASK* format. Right: case of the *CSRZ-DPSK* format for a transmission over 4000 km. The input power per channel is equal to -3 dBm.

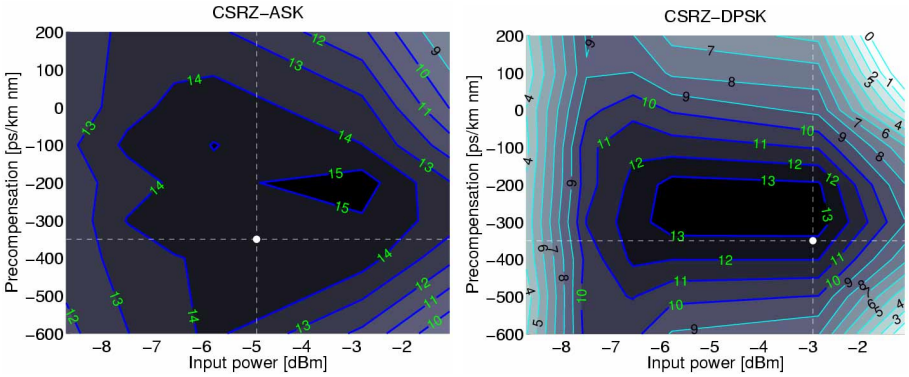

Fig 5. Left: numerical estimation of the output *Q* factor [dB] at 2000 km as a function of the pre-compensation and per-channel input power for *CSRZ-ASK* format transmission. Right: output *Q* factor at 4000 km for the *CSRZ-DPSK* format transmission.

Indeed, as we shall demonstrate in the remainder of this section, for the *DPSK* modulation format the *BER* value may only be correctly estimated by using moment generating functions and the saddle point approximation [27-28]. Nevertheless, although it is known that the *Q* factor is invalid in predicting the observed *BER* value, a first approximation to the optimization of a transmission system parameters (namely, the optimal selection of the dispersion map or span input signal power level) may be performed by using a simple estimation of the *Q* factor as shown in Fig. 4 and 5. On the other hand, Fig. 6 shows that only the statistical direct calculation of the *BER* value properly predicts the experimentally observed optimum output signal *OSNR* (or, equivalently, span input channel power level). We show by empty circles (joined by a fitting red solid curve) the experimentally measured *BER* vs. the receiver *OSNR* (in 1 nm) after a 4000 km long UltraWave^{TM} fiber link. The empty squares joined by a blue solid curve illustrate the numerically computed *BER*, obtained by the moment generating functions and the saddle point approximation, as discussed in reference [27] and implemented in the commercial software Virtual Photonics (*VPI*) Transmission Maker 7.0. In order to arrive at the direct numerical *BER* evaluation for signal transmission

#82382 - $15.00 USD Received 24 Apr 2007; revised 4 Jul 2007; accepted 15 Jul 2007; published 21 Aug 2007

over a 4000 km long UltraWave™ fiber-based link using the *DPSK* format, we numerically computed with our proprietary simulation code the propagation of the optical field throughout the entire link. The resulting optical field emerging from the receiver's optical filter was fed into the *VPI* receiver module for the direct calculation of the corresponding *BER*. For simplicity, we did not include in all of our receiver modules any electrical receiver noise.

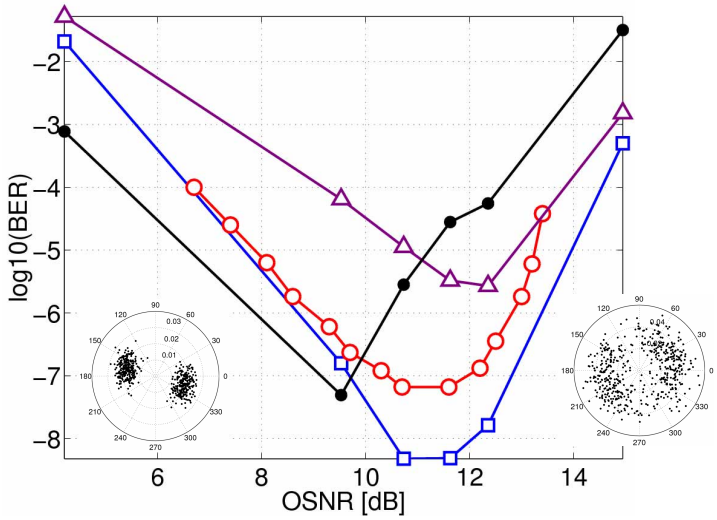

Fig 6. Comparisons of *BER* predictions (versus received *OSNR* in 1 nm after a 4000 km UltraWave™ link) and experiments for the *CSRZ-DPSK* format. △: Numerical *BER* from the *Q* factor; ○: *BER* from experiments; □: *BER* from semi-analytical approach; ● *BER* from differential phase *Q*. Insets: phasor diagrams (optical field) for input channel powers of either -6 dBm (left plot) or 0 dBm (right plot).

Next, we evaluated the Personick's amplitude *Q* factor at the output of a balanced receiver with both our own receiver module and with the corresponding *VPI* receiver module. In both cases, we obtained (via the *Q* factor and the hypothesis of a Gaussian *pdf* for the electrical current fluctuations) virtually the same *BER* estimate as a function of the output *OSNR*: this estimate is shown in Fig. 6 by the open triangles, joined by a violet solid curve. Finally, we also computed the differential phase *Q* factor, which is obtained as discussed in reference [20] from mean values and standard deviations of the phases of the optical pulses (see filled black circles joined by a black solid curve in Fig. 6). By comparing all curves in Fig. 6, it is clear that the direct *BER* calculation based on moment generating functions and the saddle point approximation compares much better with the measured *BER* (both in terms of the absolute *BER* values for all *OSNR*s, as well as in terms of the selection of the optimum output *OSNR* ~ 11.8 dB value) than the *BER* estimation based on the different *Q* factors. Indeed, the *BER* estimation based on the amplitude *Q* factor results in a minimum *BER* (or maximum *Q* value) for the output *OSNR* value of 12.5 dB, i.e., the *Q* factor estimation differs by 0.7 dB from the experimentally determined value. On the other hand, Fig. 6 shows that the differential phase *Q* factor leads to a significant under-estimation (by about 2 dB) of the optimal receiver *OSNR*. Note that in our numerical simulations we neglected, besides receiver electrical noise, the presence of both *PMD* and gain equalizers. We believe that neglecting these impairments explains the observed difference between numerical best fit (empty squares) and the experimental (empty circles) *BER* curves as shown in Fig. 6. Nevertheless, the results of Fig. 6 are important in that they show the excellent agreement between the experimental and numerical best-fit optimal *OSNR* value. Moreover, Fig. 6 also shows that a relatively good agreement exists between the predicted and the actual observed *BER* values when the semi-analytical direct *BER* estimation is carried out at the receiver. As a final remark, the phasor plots which are shown in the insets of Fig. 6 reveal that, in the case of the *CSRZ-DPSK*

#82382 - $15.00 USD Received 24 Apr 2007; revised 4 Jul 2007; accepted 15 Jul 2007; published 21 Aug 2007

modulation format, nonlinear phase noise is the main source of penalty for input powers above -1 dBm/ch, that is for *OSNR* values (1 nm calculated after 4000 km) larger than 13.5 dB.

4. Experimental results and discussion

The experimental optimization of the transmission performance involved the determination of the best pre-compensation, span input power per channel and post-compensation for the two modulation formats under study. As suggested by the numerical simulations, the optimal percentage of total span gain from either forward or backward Raman gains was fixed in the experiments to 20%-80%, and it was kept unchanged when using either the *CSRZ-ASK* or the *CSRZ-DPSK* format. Figures 7 and 8 summarise the results of our experimental optimizations. In Fig. 7(a) we show the measured *BER* for the central channel at 1550 nm, versus pre-compensation. The measurements were taken at 2000 km for the *CSRZ-ASK* format and at 4000 km for the *CSRZ-DPSK* format. In Fig. 7(b) we display the central channel *BER* versus its residual chromatic dispersion for the two modulation formats, when measured at the same transmission distances as in Fig. 7(a). Note that in Fig. 7 we used a spline fit to join the experimental points as a guide to the eye.

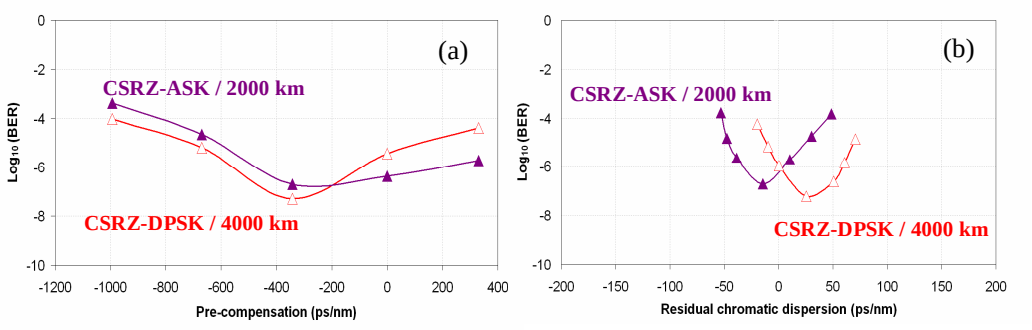

Fig 7. (a) *BER* versus pre-compensation at 2000 km for *CSRZ-ASK* and at 4000 km for *CSRZ-DPSK* for the central channel at 1550 nm, *(b) BER* versus residual chromatic dispersion of the central channel at 1550 nm at 2000 km for *CSRZ-ASK* and at 4000 km for *CSRZ-DPSK*.

From the observations of Fig. 7(a), one may notice that the same optimal pre-compensation of -350 ps/nm holds for both the *CSRZ-ASK* and *CSRZ-DPSK* modulation formats. Note that in the measurements of Fig.7(a) and (b) the span input power per channel was kept fixed to -5 dBm for the *CSRZ-ASK* format and to -3 dBm for the *CSRZ-DPSK* format. The results of Fig. 7(a) also show that the observed optimal negative values of pre-compensation are in good agreement with the simulation predictions of Fig. 4. On the other hand, Fig. 7(b) shows that it is necessary to accurately adjust the post-compensation in order to improve the transmission performance for the central channel by means of a proper control of the residual chromatic dispersion (with the pre-compensation fixed to -350 ps/nm). We achieved this optimal post-compensation by means of our *TDCM*. Figure 7(b) shows that the optimal residual dispersion for the central channel remains close to 0 ps/nm: in particular, the residual dispersion is slightly positive (+25 ps/nm) for the *CSRZ-DPSK* format, and it is slightly negative (-15 ps/nm) for the *CSRZ-ASK* format. In the following, we kept fixed the pre-compensation at its optimal value of -350 ps/nm for both modulation formats.

Figures 8(a) and (b) show the output *BER* as a function of the span input power per channel for the *CSRZ-ASK* and the *CSRZ-DPSK* formats. The *BER* was measured at various transmission distances (as indicated on the plots of Fig. 8(a) and (b)). As it can be seen in Fig.(8), at 4000 km with the *CSRZ-DPSK* format the optimal span input power is about 2 dB larger than at 2000 km with the *CSRZ-ASK* format (i.e., -3 dBm against -5 dBm); whereas the *BER* is nearly the same (~10^{-7}) in the two cases. We may also observe from Fig. 8(a) that the optimal span input signal power with the *CSRZ-ASK* format significantly changes with the

#82382 - $15.00 USD Received 24 Apr 2007; revised 4 Jul 2007; accepted 15 Jul 2007; published 21 Aug 2007

transmission distance.

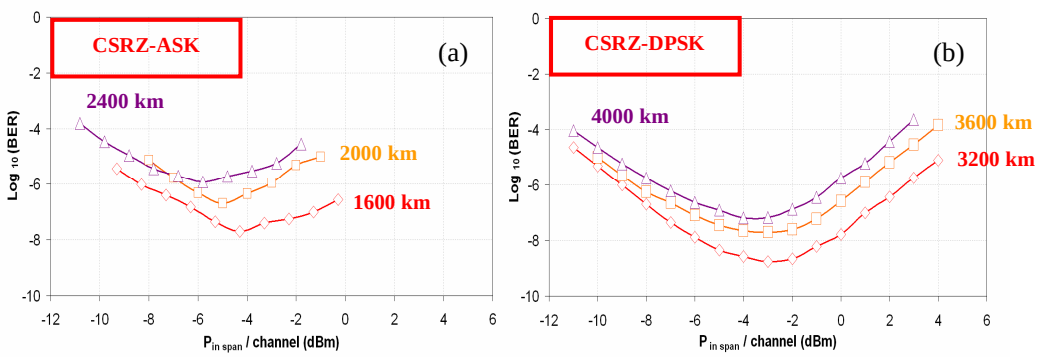

Fig 8. (a) *BER* versus span input power of the central channel at 1550 nm at different transmission distances for *CSRZ-ASK, (b) BER* versus span input power of the central channel at 1550 nm at different transmission distances for *CSRZ-DPSK*.

Indeed, the optimal input power with the *CSRZ-ASK* decreases by about 1 dB per additional signal circulation through the loop. On the other hand, Fig. 8(b) shows that, when using the *CSRZ-DPSK* format, the transmission distance dependence of the optimal span input power per channel is significantly reduced. These measurements confirm that the *CSRZ-ASK* modulation format is largely more sensitive to the accumulation of nonlinear impairments than *CSRZ-DPSK* [20-22]. Indeed, it is well known that the main sources of nonlinear degradation for pulse-overlapped 40 Gb/s optical transmissions are intra-channel cross-phase modulation (*IXPM*) and intra-channel four-wave mixing (*IFWM*). In *ASK* transmission, *IXPM* and *IFWM* lead to pulse timing and amplitude jitters for the marks, and to "ghost" pulse generation in the spaces [22]. It is also established that a symmetric dispersion map (as the one which is implemented in the present experiments) significantly improves the performance of *ASK*-based transmissions [23], by limiting the impact of both *IXPM* and *IFWM*. Nonetheless, when using the *DPSK* format over the same symmetric dispersion map, one obtains a net reduction of the overall intra-channel nonlinear impairments as compared with the *ASK* format. First of all, it is clear that for a given level of the signal average power the pulse peak power with the *DPSK* format is twice lower than with the *ASK* format. Moreover, the Gordon-Mollenauer effect [24] which is responsible for a detrimental nonlinear phase noise with the *DPSK* format, may be highly reduced in a pulse-overlapped 40 Gb/s transmission owing to the strong impact of dispersive effects (as it is the case in the present transmission line owing to the high local dispersion of the *SLA* and *IDF* fibers). Finally, note that *IFWM* has only limited influence on *DPSK* transmissions: indeed the *IFWM*-induced nonlinear phase noise leads to a correlation between the nonlinear phase shifts that are experienced by any two adjacent bits [20-21]. Clearly this does not affect the information which is contained, for the *DPSK* format, in the relative phase difference between bits [20-21]. Figure 9(a) shows the measured dependence of the output *OSNR* (measured for the central channel in 1 nm) and *BER* versus the transmission distance for both the *CSRZ-ASK* and the *CSRZ-DPSK* formats. In these measurements, for each transmission distance we adjusted the span input power and the post-compensation to their optimal values. On the other hand, in Fig. 9(a) the pre-compensation was not changed with respect to the value that was previously obtained by optimising the transmission performance as in Fig. 7(a) (at 2000 km for the *CSRZ-ASK* and at 4000 km for the *CSRZ-DPSK* format). As it can be seen in Fig. 9(a), for a

#82382 - $15.00 USD Received 24 Apr 2007; revised 4 Jul 2007; accepted 15 Jul 2007; published 21 Aug 2007

given level of the output *BER*, the *DPSK* format enables a dramatic increase of the transmission distance with respect to the *ASK* format. Namely, for a $BER=10^{-10}$ the transmission distance grows from 800 km (with the *ASK*) up to 2400 km (with the *DPSK*). For a $BER=10^{-9}$ one obtains 1200 km with the *ASK* format and 3200 km with the *DPSK* format.

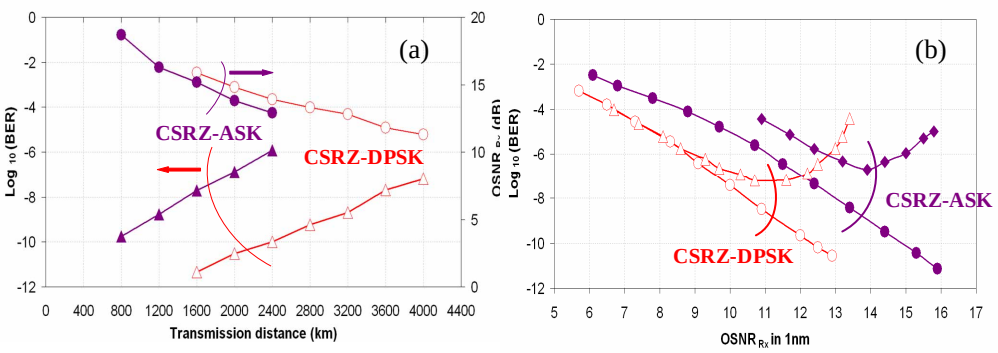

Fig 9. (a) *BER* and *OSNR* of the central channel at 1550 nm versus transmission distance for *CSRZ-ASK* and *CSRZ-DPSK*, *(b) BER* versus *OSNR* of the central channel at 1550 nm after 2000 km for *CSRZ-ASK* (filled purple lozenges) and after 4000 km for *CSRZ-DPSK* (empty red triangles) and in back-to-back for the both modulation formats (filled purple circles for *CSRZ-ASK* and empty red circles for *CSRZ-DPSK*).

For a $BER=10^{-8}$, Fig. 9(a) shows that one obtains 1600 km with the *ASK* and 3600 km with the *DPSK*. Finally, for a $BER=10^{-7}$, we obtain a transmission distance of 2000 km with the *ASK* and of 4000 km with the *DPSK* format, respectively; that is, in this case the *CSRZ-DPSK* modulation format permits to double the transmission distance when compared with *CSRZ-ASK*. Figure 9(a) also shows that the output *OSNR* is equal to 13.8 dB at 2000 km (for the *ASK* format) and to 11.3 dB at 4000 km for the *DPSK* format, respectively. Although the output *OSNR* is 2.5 dB lower with the *CSRZ-DPSK* format at 4000 km when compared with the case of the *ASK* format at 2000 km, nevertheless one obtains the same *BER* performance (10^{-7}) in the two cases. The superior behaviour of the *DPSK* format can be mostly ascribed to its well-known 2.5-3 dB improvement in receiver sensitivity with respect to the *ASK* format (such improvement was clearly observed on the back-to-back sensitivity curves as shown in Fig. 9(b)). Additionally, as discussed above the resilience of the DPSK format to nonlinear impairments is higher than that of the *ASK* format [20-21]. Let us point out that the results of the experimental optimization fit well the numerical results that we described in section 3: for both the *ASK* and the *DPSK* modulation formats, numerical predictions agree well with experimental optimal span input power per channel values. At last, note that the *BER* level ($=10^{-7}$) which is obtained at 2000 km and 4000 km (for the *CSRZ-ASK* and the *CSRZ-DPSK* formats, respectively) is well below the threshold for error-free operation of forward error correction codes (which is in the *BER* range of $[1.10^{-3}\text{-}4.10^{-3}]$, depending of the equipment supplier which is considered), proving that on UltraWave™ fiber both *CSRZ-ASK* and *CSRZ-DPSK* modulation formats respond to the requirement of carriers' core transport network for *ULH* transmissions reaching more than 2000 km.

In Fig. 9(b) we show the results of the comparison of the dependence of the output *BER* upon the received *OSNR* for both the *ASK* and the *DPSK* formats. The *OSNR* was measured in 1 nm for the central channel at 1550 nm, both in back-to-back and after transmission (over 4000 km for the *CSRZ-DPSK* and 2000 km for the *CSRZ-ASK* format, respectively). Clearly, the received *OSNR* is a monotonic increasing function of the span input power. Therefore,

#82382 - $15.00 USD Received 24 Apr 2007; revised 4 Jul 2007; accepted 15 Jul 2007; published 21 Aug 2007

qualitatively similar plots to those in Fig. 9(b) result when one displays the output *BER* versus the span input power per channel. However, the advantage of showing the dependence of the ouput *BER* versus the received *OSNR* is that one may directly read from the plot of Fig. 9(b) the *OSNR* transmission penalty, by simply comparing the back-to-back *OSNR* value with that obtained after the transmission (for the same level of *BER*). The *BER* versus *OSNR* curves in Fig. 9(b) that are obtained after transmission clearly show that at low *OSNRs* (or, equivalently, low span input powers) the accumulated amplified spontaneous emission (*ASE*) noise sets the limit to the transmission performance. Whereas the same curves in Fig. 9(b) also show that at high *OSNRs* the transmission quality is mostly deteriorated by nonlinear impairments. Clearly, the optimal working point (and minimum BER level) is obtained when *ASE* and nonlinearities contribute to transmission penalties in equal manner. By comparing in Fig. 9(b) the back-to-back *BER* curves with those obtained after transmission, one obtains that, at the above discussed optimal working point (i.e., *OSNR* value that yields minimum *BER*, which in the case of Fig. 9(b) is equal to 10^{-7} for both modulation formats), the *OSNR* penalty is equal to 1 dB at 4000 km for the *CSRZ-DPSK* format, and to 2 dB at 2000 km for the *CSRZ-ASK* format. Namely, with the *DPSK* format we observed 1dB of transmission impairment reduction with respect to the *ASK* case, in spite of the doubled transmission distance. It is interesting to note that the well-known ~2.5 dB *OSNR* sensitivity difference between the *CSRZ-ASK* and the *CSRZ-DPSK* modulation formats that is obtained in back-to-back (at the *BER* level of 10^{-7}) is maintained nearly unchanged after signal transmission over either 2000 km or 4000 km, respectively. Note finally that we measured the *BER* of all the sixteen channels in both transmission configurations (i.e., *CSRZ-ASK* over 2000 km and *CSRZ-DPSK* over 4000 km). The resulting observed *BER* for all these channels was varying within 1 decade around the *BER* value that we obtained for the central channel.

5. Conclusion

We carried out a detailed experimental optimization and comparison of the performance of *ULH WDM* 40 Gb/s transmissions using either the *CSRZ-ASK* or the *CSRZ-DPSK* modulation format. We revealed that, for properly optimized systems, the error-free transmission distance with the *CSRZ-DPSK* format basically doubles the system reach with respect to the *ASK* format. Moreover, in our optimal configuration the well-known 2.5-dB receiver sensitivity advantage of *DPSK* which is observed in back-to-back is maintained unchanged after transmission. The observed results were closely reproduced by numerical fits of the experiments. In particular, we experimentally verified that in our system the semi-stochastic *BER* estimator using moment generating functions and the saddle point approximation [26] is better suited to predict both the *BER* level and the optimal working point when using the *CSRZ-DPSK* modulation format. Our study of the critical assessment and comparison of the performance of *ULH WDM* 40 Gb/s systems based on the UltraWave™ fiber represents a sort of reference case, to be extended in future work to links based on the G.652 standard single mode fiber (which is today's most deployed fiber worldwide) or on G.655 non-zero dispersion-shifted fibers.

Acknowledgments

The authors want to acknowledge particularly *OFS Fitel* for loaning us the UltraWave™ fiber and J. Steenstrup for his kind support.

#82382 - $15.00 USD Received 24 Apr 2007; revised 4 Jul 2007; accepted 15 Jul 2007; published 21 Aug 2007